Tailoring the Synthesis and Heating Ability of Gold Nanoprisms for Bioapplications

Beatriz Pelaz[†], Valeria Grazu[†], Alfonso Ibarra[‡], Cesar Magen[‡,§,⊥], Pablo del Pino*[,†,⊥] and Jesus M. de la Fuente*[,†,§]

[†] Instituto de Nanociencia de Aragon (INA), Universidad de Zaragoza, 50018 Zaragoza, Spain, [‡] Laboratorio de Microscopias Avanzadas (LMA) – Instituto de Nanociencia de Aragon (INA), Universidad de Zaragoza, 50018 Zaragoza, Spain, [§] Fundacion ARAID, 50004 Zaragoza, Spain, [⊥] Departamento de Fisica de la Materia Condensada, Universidad de Zaragoza, 50009 Zaragoza, Spain

S1) Time evolution of the reaction to produce NPs

Within the first 5 minutes of the reaction, the color of the solution changed gradually from yellow (gold salt) to brownish. Typically, this is an indication of the formation of Au NPs. At this early stage of the reaction, 1 mg of HS-PEG-COOH was added to 1 mL of the initial mixture. We added such an excess of thiolated polymer to prevent further growth of NPs. The UV-Vis-NIR spectra of the solution before and after the addition of thiolated PEG exhibited the same features (data not shown). This is indicative that the reaction was successfully stopped. Figure S1 shows a representative TEM image of the "frozen" products obtained within the initial stage of the reaction. Figure S1 revealed the presence of small NPs (diameter less than 3 nm), polyhedral Au NPs (diameter less than 15 nm) and mainly, Au nanoprisms (edge length less than 35 nm). We called these initial NPs "seeds" because the final products of the synthesis route proposed leaded to "grown seeds", i.e. polyhedral Au NPs (diameter of 30 nm) and NPRs (edge length of 100-200 nm).

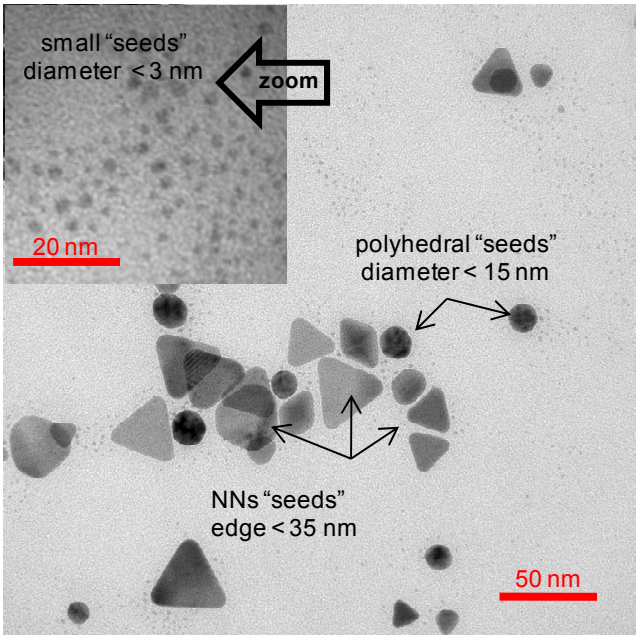

Figure S1. TEM image of the "frozen" products obtained within the first 5 minutes of the reaction. Arrows point at different NPs, i.e. NPRs "seeds", polyhedral "seeds" and small "seeds". Inset shows a magnification of a region of the TEM-grid containing small "seeds"

S2) Electron Microscopy Characterization

As we discussed in the manuscript, the edge length of NPRs increased as the volume of the second addition of reductant increased (from 0.2 *x* to 0.5 *x*). Low magnification FE-SEM images and the corresponding histograms representing the size distribution of the different preparations are shown in Figure S2–1.

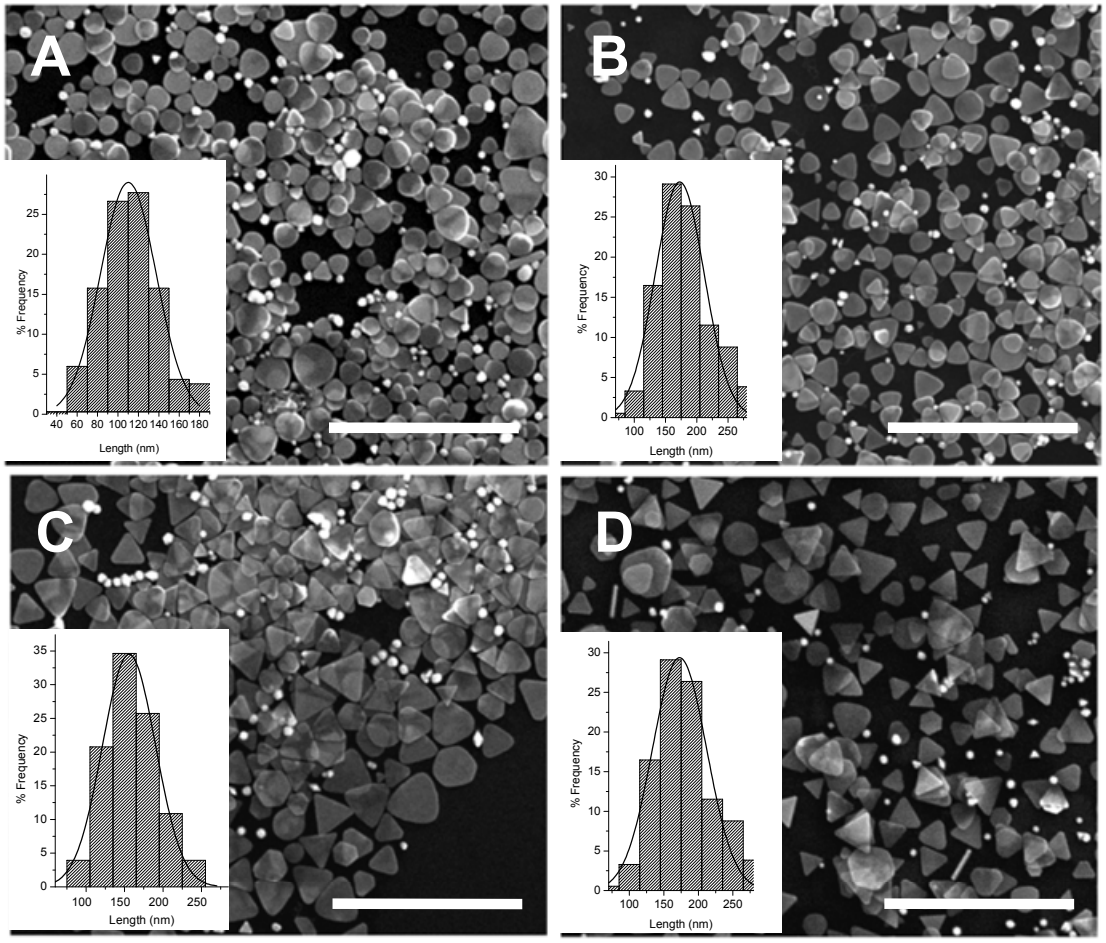

Figure S2–1. SEM images of each reported NPRs@PEG, i.e. A) 0.2 *x*, B) 0.3 *x*, C) 0.4 *x* and D) 0.5 *x*. Insets show the corresponding histograms (over more than 300 NPs) representing the size distribution of different NPRs. Scale bars are 1 μm in all cases.

As we discussed in the manuscript, all synthesis methods to produce gold nanoprisms tend to yield some small percentage of tip-truncated nanoprisms or nanodisks. High magnification of selected STEM images shown in Figure S2–2 highlight this fact which becomes more apparent as the edge length of NPRs decreases; panel (A) shows the predominant disk-like morphology of NPRs with an average edge length of 104.5 ± 32 nm (note that this length can be measured from tip to tip of the NP because the triangular shape still is discernible); the NPRs in panel (B) with edge length 127.6 ± 40 nm still show disk-like shape although to a lesser extent than NPs in panel (A); in panel (C), for NPRs with average edge length 146.9 ± 35 nm, the rounded-tips and edges are still discernible; finally, NPRs in panel (D) with average edge length 165.3 ± 42 nm show regular edges even though due to tip-truncation some NPs appear to have hexagonal top/bottom faces.

The flat morphology of NPRs was studied by TEM tilt series. Figure S2–2 (E) shows the side view of a NPR (surrounded by polyhedral NPs) which apparently resembles the shape of a rod. However, a TEM image of the same group of NPs with the specimen tilted about 30º revealed the prismatic nature of the NPR (Figure S2–2 (F)). Indeed, STEM images shown in Figure S2–2 (G, G, and I) exhibit the presence of apparently rod-like NPs with constant thickness (9 nm) which correspond to the side view of NPRs.

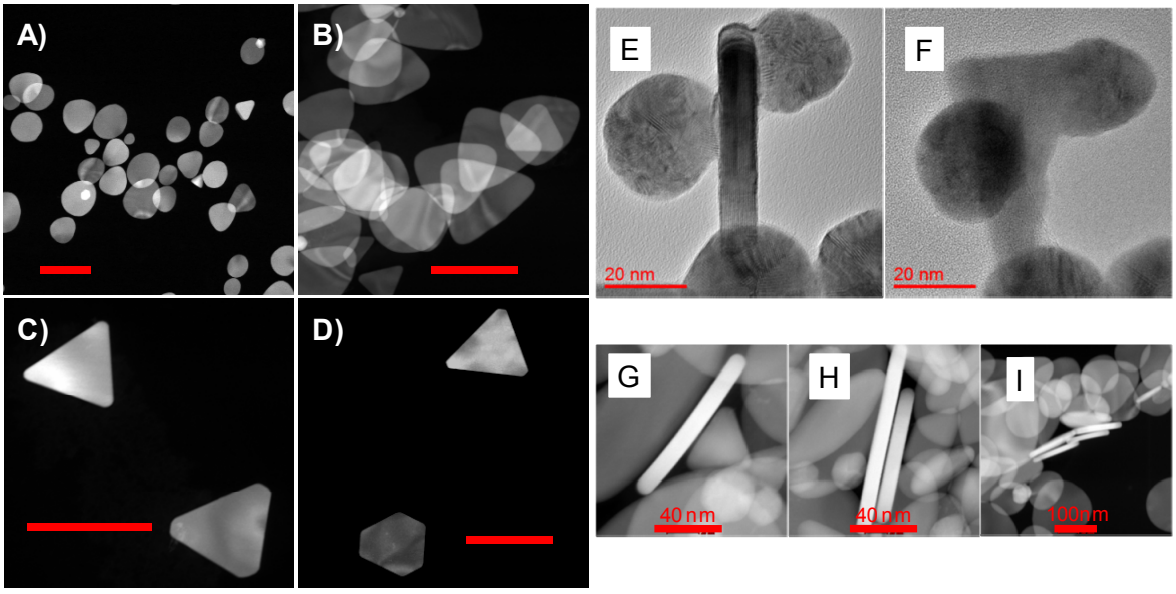

Figure S2–2. Selected STEM images of each reported NPR, i.e. A) 0.2 *x*, B) 0.3 *x*, C) 0.4 *x* and D) 0.5 *x*. Scale bars are 200 nm in all panels. HR-TEM images of (E) the side view of a NPR and (F) the corresponding image of the tilted specimen showing the prismatic morphology of the NP. HR-STEM images of selected samples (G, H and I) where the flat shape and constant thickness of NPRs is apparent.

EELS thickness analysis indicated that a uniform thickness of approximately 9 nm is conserved among different preparations. This is supported by the STEM-HAADF images, where contrast uniformity in flat NPRs indicates the same thickness. Different EELS thickness maps shown in Figure S2–3 measure the sample thickness homogeneity in the reported samples.

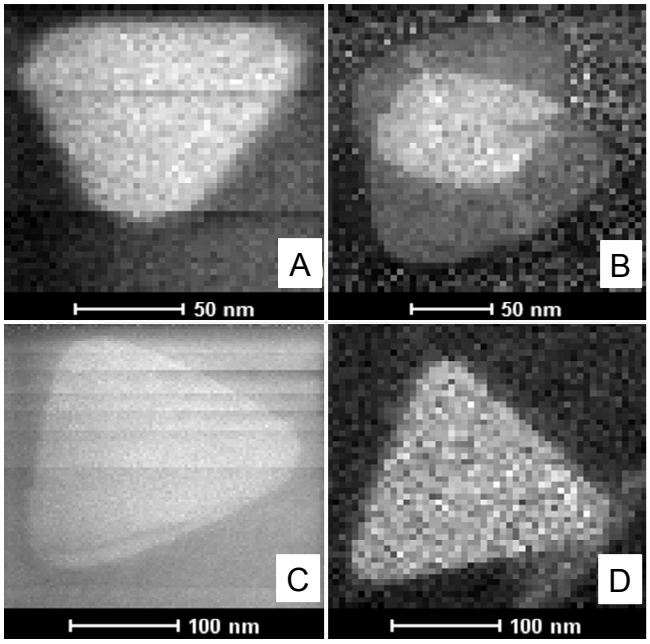

Figure S2–3. EELS thickness map of each reported NPR, i.e. A) 0.2 *x*, B) 0.3 *x*, C) 0.4 *x* and D) 0.5 *x*.

S3) MTT assay

Cell viability and proliferation were analyzed by MTT colorimetric assay. VERO cells (5×10^3 cells per well) were seeded in a 96 well plate at 37 °C in 5% CO_2. After 24 h, the medium was replaced with fresh medium containing different types of NPRs (bare, PEG, and PEG derivatized with the dye TAMRA and glucose) in varying concentrations (50, 100 and 200 $\mu g\times mL^{-1}$). Cells were challenged with NPRs for 24 hours in the incubator; then, NPRs solutions were removed and cells were washed with PBS; 20 μL of 3-(4,5-dimethylthiazol-2-yl)-2,5-diphenyltetrazolium (MTT) dye solution (5 $mg\times mL^{-1}$ in PBS) solved in 100 μL of DMEM media were added to each well. After 2 hours of incubation at 37 °C and 5% CO_2, cells were centrifugated at 5000 rpm for 10 minutes and the medium was removed. Formazan crystals were dissolved in 100 μL of DMSO. The absorbance of each well was read on a microplate reader (D Biotek ELX800) at 570 nm. The spectrophotometer was calibrated to zero absorbance using culture medium without cells. The relative cell viability (%) related to control wells containing cell incubated without NPRs was calculated by [*A*]test/[*A*]control*100. Each measurement was repeated at least five times to obtain the mean values and the standard deviation. The following graph (Figure S3) demonstrates that different types of NPRs do not impair cell viability at NPRs concentrations up to 200 $\mu g\times mL^{-1}$.

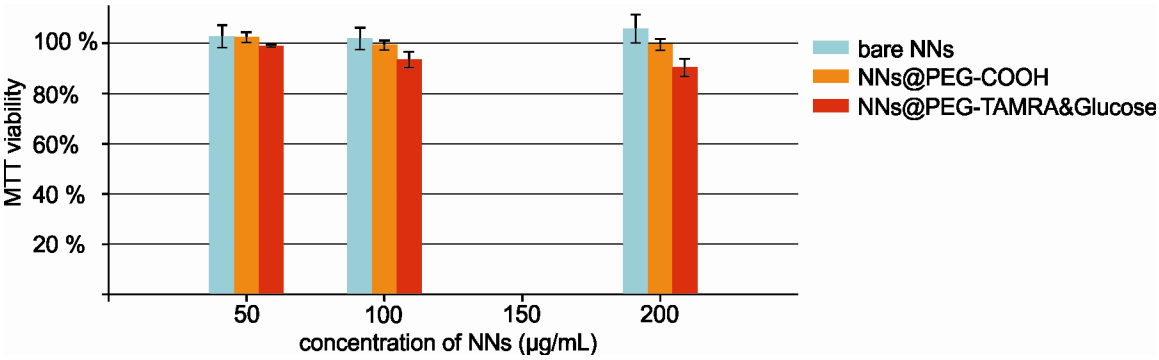

Figure S3. MTT viability (VERO cells) with NPRs of the types: bare, pegylated and functionalized with TAMRA and glucose.

S4) Irradiation and Live/Death Assay

Vero cells (kidney epithelial cells of an African green monkey) were cultured in µ-Dishes from Ibidi (3.5 cm^2, ibiTreat coated for optimized adhesion of most cell types). Cells were grown for 24 hours prior to addition of NPs; then, cells were supplemented with previously sterilized NPRs@ PEG-TAMRA&Glc to a final concentration of 0.1 $mg \times mL^{-1}$. Cells were challenged with functional NPRs for 8 hours; then, cells were washed out of non-internalized NPRs and washed with PBS. For the experiment shown in Figure S4-1, cells were stained for the nucleus DNA with Blue Hoechst dye. Cells filled with functional NPRs were then used for local NIR irradiation (*ca.* 30 $W \times cm^{-2}$; 2 minutes) and observed under an inverted fluorescence microscope immediately after laser exposure. Figure S4-1 shows the effect of laser irradiation; in the right panel (bright field image), the effect of laser irradiation is apparent; also, in the right panel (merged image from blue and red fluorescence channels) functional NPRs (red fluorescence) escaped from irradiated cells, probably, due to membrane damage, whereas cells in the non-illuminated regions kept NPRs.

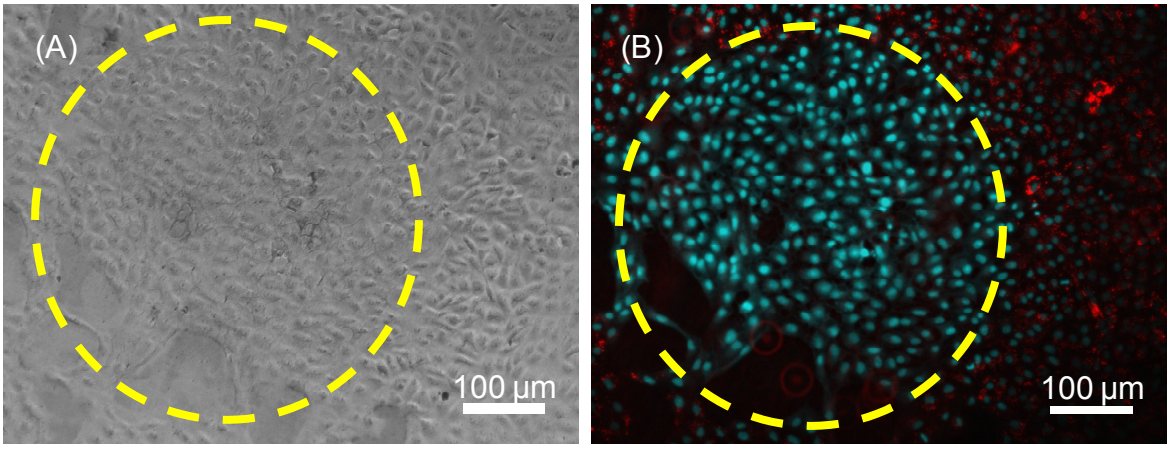

Figure S4-1. (A) Bright field (BF) image of cells filled with NPRs@PEG-TAMRA&Glc were exposed to laser irradiation; (B) corresponding fluorescence image (red and blue fluorescence corresponding to NPRs and nuclei, respectively). Scale is 100 µm in both panels. The yellow dashed circle represents the laser spot.

In a complementary experiment, cells with and without NPRs (control experiment) were cultured and irradiated as in the experiment described previously (Figure S4-1). Then, cells were incubated for 12 extra hours before studying their viability with the Live/Dead test from Invitrogen. In the control experiment where cells were cultured in the absence of NPRs (Figure S4-2), cells are 100% viable since all cells are green (Calcein AM) stained and there is not sign of cell damage in the BF or fluorescence merged image.

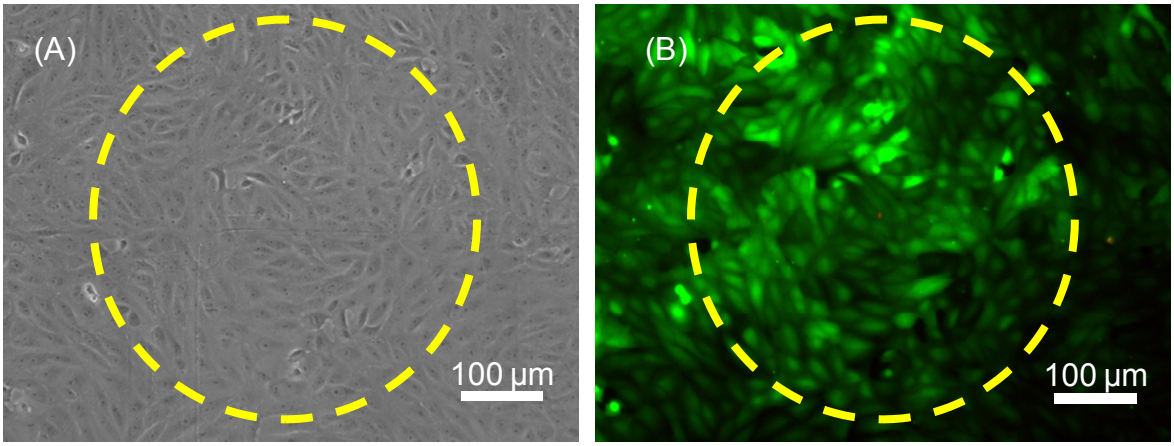

Figure S4-2. (A) Bright field and (B) corresponding fluorescence merged image of green and red channels corresponding to Calcein AM (viable cells) and EthD-1 (dead cells). The yellow dashed circle represents the laser spot.

In contrast, for the cells cultured in the presence of NPRs, the damage is apparent in the BF image and fluorescence merged images (Figure S4-3). Panels (C) and (D) show a zoomed area of the region irradiated region in panels (A) and (B).

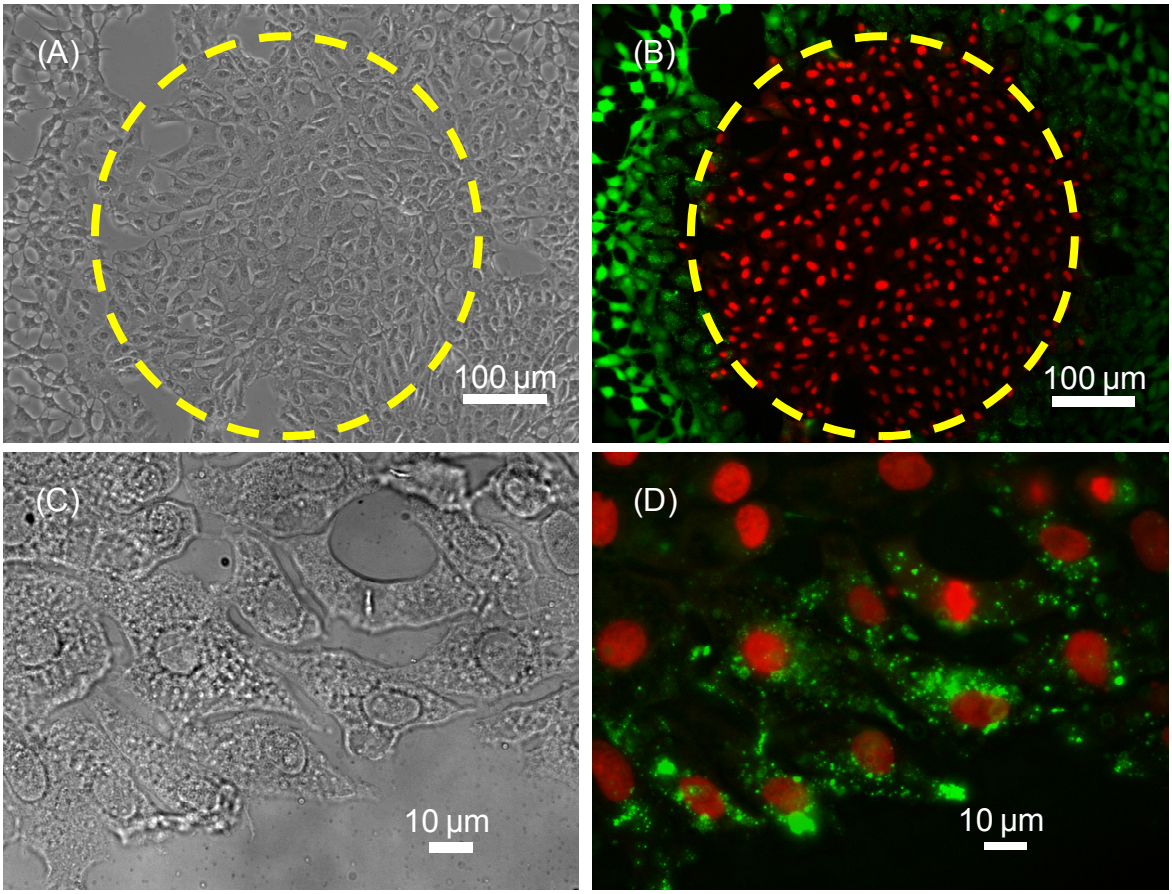

Figure S4-3. (A) Bright field and (B) corresponding fluorescence merged image of green and red channels corresponding to Calcein AM (viable cells) and EthD-1 (dead cells). Panels (C) and (D) are the BF and fluorescence images of a zoomed area of irradiated cells. The yellow dashed circle represents the laser spot.